CHEMISTRY
A EUROPEAN JOURNAL

DOI: 10.1002/chem.200800837

Steric Effects in RNA Interference: Probing the Influence of Nucleobase Size and Shape

Alvaro Somoza, Adam P. Silverman, Rand M. Miller, Jijumon Chelliserrykattil, and Eric T. Kool*[a]

Abstract: Nonpolar nucleosides with varying size and shape have been used to study the hydrogen-bonding stabilization and steric effects on RNA interference. The uracil and adenine residues of siRNA guide strands have been replaced by nonpolar isosteres of uracil and adenine and by steric variants. RNAi experiments targeting *Renilla* luciferase mRNA have shown close correlation between siRNA thermal stability and gene suppression. Interestingly, siRNA modified at position 7 on the guide strand does not follow this correlation, having substantial RNAi activity despite low thermal stability. Sequence-selectivity studies were carried out at this position with mutated target mRNAs and nucleobase analogues with varied size (2,4-difluoro- and 2,4-dichlorobenzene) and different shape (2,3-dichlorobenzene, 4-methylbenzimidazole). The results point out the importance of nucleobase shape and steric effects in RNA interference.

Keywords: base pairs · nucleobases · RNA recognition · RNA structures

Introduction

RNA interference (RNAi) has become an essential tool for studying gene function in biological and biomedical research by specifically silencing a targeted gene.[1] This process is commonly triggered by double-stranded RNA of 21–23 nucleotides with two nucleotides overhanging (DT),[2] although different length and structures, such as hairpins[3] or blunt-end duplexes,[4] can be employed as well. These short RNA duplexes are known as small-interfering RNAs (siRNAs). The two strands of the duplexes have different significance: one is responsible for recognizing the target mRNA sequence (the guide strand), while the complementary strand has no key role in the recognition and is known as the passenger strand.

The RNAi pathway is initiated when a siRNA reaches the cytoplasm and a protein complex known as RISC (RNA-induced silencing complex) binds the siRNA duplex.[5] The RISC complex selects the strand 5′ end with lowest thermal stability in the duplex by using the RD2D2 protein.[6] In this way, the guide strand is incorporated into the active RISC complex; meanwhile the passenger is cleaved and released to the cytoplasm.[7] The guide strand in the RISC complex serves as template to localize the complementary mRNA in the cytoplasm. Once the guide strand binds the targeted mRNA, the target is cleaved due to the RNAse activity present on the PIWI domain of the RISC complex.[8] The mRNA fragments are released to the cytoplasm and the RISC complex repeats this process, cleaving more target mRNAs.

The catalytic mechanism involved and the high specificity achieved by sequence complementarity make this process a powerful tool for the control of gene expression. For these reasons it has been considered a potential strategy for targeted therapy, since the expression of proteins involved in diseases can be selectively inhibited. However, there are still several drawbacks to overcome, such as off-target effects,[9] stability in serum,[10] and biodistribution.[11] In this context, a variety of chemically modified siRNAs has been studied in an effort to address these limitations.[12] Most of the modifications have been incorporated or attached on the passenger strand, since this strand is degraded during RISC activation and does not interfere in the process. These modifications are intended to provide higher stability in serum and better biodistribution, such as the use of cholesterol on the 3′ end reported by Soutschek et al.[13] Modifications on the guide strand are more problematic, since they may directly inhibit the RNAi activity. However, selected modifications at spe-

[a] Dr. A. Somoza, Dr. A. P. Silverman, R. M. Miller, Dr. J. Chelliserrykattil, Prof. Dr. E. T. Kool
Department of Chemistry, Stanford University
Stanford, CA 94305–5080 (USA)
Fax: (+1) 650-725-0259
E-mail: kool@stanford.edu

Supporting information for this article is available on the WWW under http://dx.doi.org/10.1002/chem.200800837.

cific positions of the guide strand can have interesting effects. Modifications on the sugar moiety, particularly on the 2′-hydroxyl groups, provide enhanced resistance to nucleases[14] and can reduce off-target effects.[12c,15] Moreover, the use of chemically modified nucleotides has been essential for the study of the mechanism of RNAi,[16] providing fundamental knowledge for the efficient design of siRNAs.[17]

Despite the significant contributions focused on understanding the RNAi process and developing therapies based on RNAi, the RISC-mediated siRNA-target interaction is not completely understood yet, and simple nucleic acid hybridization does not explain target recognition.[18] The interactions that take place inside the RISC complex (protein–siRNA–mRNA) are key in target recognition, and better understanding of these interactions is required for optimal design of siRNAs.

In connection with our program devoted to studying the role of electrostatics and sterics in biological systems,[19] and due to the significance of the RNA interactions inside the RISC complex, we have undertaken studies to evaluate the roles of these molecular properties on the RNAi process. In an early study we previously reported the effect on RNAi activity of uracil replacement by its nonpolar isostere 2,4-difluorobenzene (rF).[20] In that case, the gene supression activity was retained in several modified siRNAs despite the lack of hydrogen bonding stabilization. In particular, position 7 of the guide strand was surprisingly insensitive to this substitution, yielding significant RNAi activity despite low thermal stability compared with the wild-type duplex. Simultaneous studies by Manoharan also found a similar effect.[21] In our study, selectivity studies at this position employing singly mutated target mRNAs showed that the nonpolar isostere retained the selectivity of uracil. This led to the hypothesis that sequence selectivity might arise from protein-enforced steric effects.

In this new work, we test this hypothesis by studying nonpolar nucleobase analogues of varied size and shape. We report the synthesis of modified phosphoramidites and their use in RNAi experiments, evaluating biological activity and sequence specificity. In addition we have tested effects in a second target mRNA sequence to evaluate generality. The results provide new insights on the influences of sterics and hydrogen bonding stabilization on RNAi, and they confirm that nucleobase shape and size can play strong roles in the sequence specificity of RNAi.

Results and Discussion

Synthesis of modified nucleosides and RNAs: The halogenated nucleosides (rF, rL, rZ, and 2,3-rL) were prepared by addition of the corresponding aryllithium species to the benzyl-protected ribonolactone **1**. Stereoselective reduction was performed with triethylsilyl hydride in the presence of $BF_3{\cdot}OEt_2$, giving rise to the corresponding β-anomer derivatives (**2**–**4**). Deprotection of the benzyl groups by using BBr_3 at −78 °C afforded the free nucleosides (Scheme 1).

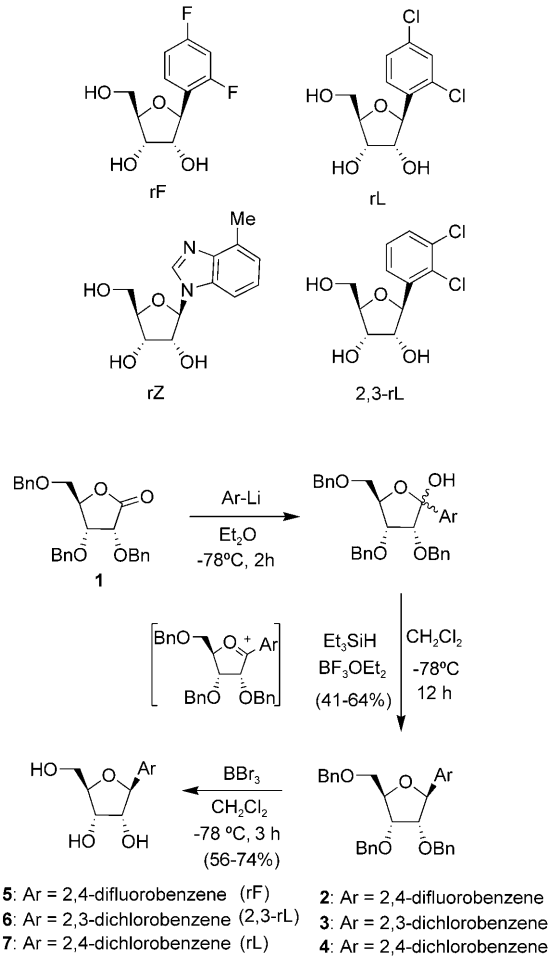

Scheme 1. Synthesis of nonpolar C-ribonucleosides. Bn = benzyl.

The free nucleosides **5–7** were then functionalized for RNA synthesis on an automated synthesizer. The 5′-hydroxyl group of the nonpolar nucleosides was protected as a dimethoxytrityl ether (DMTr) under the standard conditions. Further protection of the 2′-hydroxyl groups was carried out using the [(triisopropylsilyl)oxy]methyl group (TOM) in a standard two-step process.[22] As is commonly observed, addition of the protecting reagent TOMCl gave rise to a mixture of 2′- and 3′-TOM derivatives, in which the desired 2′-*O*-TOM was the major compound (Scheme 2).

The 4-methylbenzimidazole free ribonucleoside **8** was obtained as reported[23] and functionalized in the same way as the halogenated analogues. In this case the TOM protection gave rise to a 1:1 mixture of 2′- and 3′-derivatives.

In the case of the dichloro analogues, the 2′-*O*-TOM derivative was easily isolated by silica column chromatography. In contrast, the difluoro analogue required further manipulations to obtain the 2′-TOM-protected nucleoside in a pure form. The previously obtained mixture was treated with acetic anhydride and triethylamine, leading to the corresponding mixture of acetylated derivatives. In this case, the mixture could be easily purified by silica chromatography. The desired 2′-TOM nucleoside was finally obtained by de-

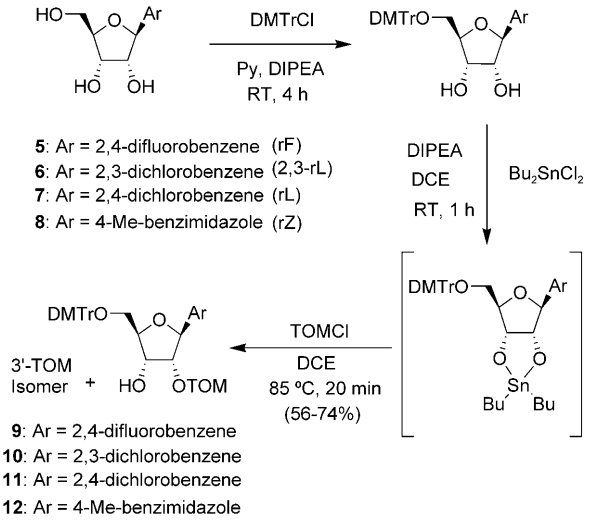

Scheme 2. Protection of free nucleosides. DMTr = 4,4′-dimethoxytrityl; Py = pyridine; DIPEA = diisopropylethylamine; DCE = 1,2-dichloroethane; TOM = [(triisopropylsilyl)oxy] methyl.

protection of the acetyl group by using ammonia in methanol. The isolation of the 2′-TOM-protected benzimidazole derivative was also difficult, but in this case the derivatization of the remaining hydroxyl groups to acetyl or isobutyl groups did not provide significant improvement in the purification. The desired isomer was ultimately obtained by repeated silica column chromatography.

The final step was the activation of the 3′-hydroxyl group as the cyanoethylphosphoramidite, required for the formation of the phosphodiester internucleotide bond during the RNA synthesis. The addition of 2-cyanoethyl-*N*,*N*-diisopropyl-phosphonamidic chloride and diisopropylethylamine afforded the corresponding phosphoramidite derivatives, which were utilized on an automated synthesizer for their incorporation into RNA (Scheme 3).

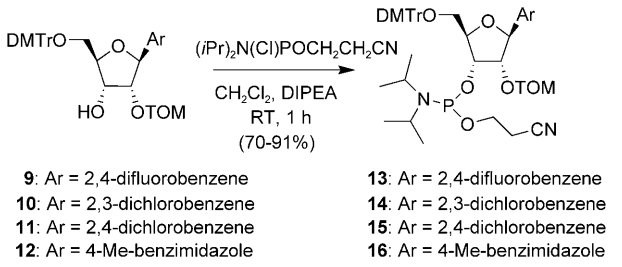

Scheme 3. Synthesis of nonpolar nucleoside phosphoramidites. Ac = acetyl, DMTr = 4,4′-dimethoxytrityl; DIPEA = diisopropylethylamine; TOM = [(triisopropylsilyl)oxy] methyl.

The modified nucleosides rF, rL, 2,3-rL, and rZ were successfully incorporated at position 7 of a 21 mer RNA guide strand of the siRNA duplex utilized in our early report (Figure 1) and characterized by MALDI-TOF mass spectrometry after PAGE purification. The siRNAs were designed to target the fragment 501–519 of *Renilla* luciferase, which was efficiently inhibited by an unsubstituted siRNA.[24]

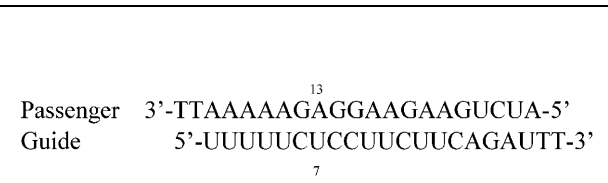

Figure 1. Wild-type siRNA duplex used to target the *Renilla* luciferase mRNA. Positions 7 (guide) and 13 (passenger) (at which substitutions were made) are numbered.

Duplex stability: First we investigated the effect of altered nucleobase shapes and sizes on siRNA duplex stability. The three halogenated benzenes were evaluated as a closely related set. The thermal stability of the duplexes was measured by using the wild-type and singly mismatched passenger strands, allowing selectivity to be evaluated. The adenine at position 13 (opposite the modified bases) was replaced by C, G, and U in the mismatched strands. The results of the studies are graphically depicted in Figure 2.

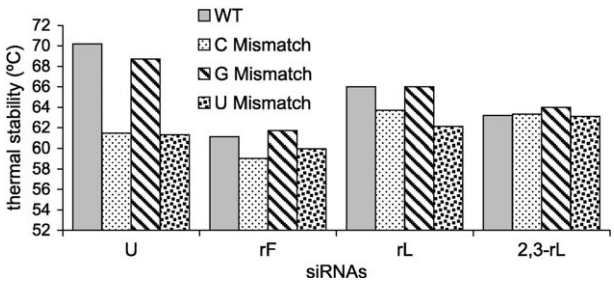

Figure 2. Thermal stability of matched and mismatched duplexes. The mismatches are at position 13 on the passenger strand. The guide strands are natural ("U") and modified at position 7 with nonpolar derivatives ("rF", "rL" and "2,3-rL"). WT = wild-type.

Overall, the nonpolar analogues at position 7 were destabilizing and showed little if any selectivity, in contrast to natural uracil. The wild-type guide strand (U at position 7) showed strong destabilization for the C:U and U:U mismatches, but in the case of the G:U mismatch the thermal stability was close to that of the canonical base pair A:U, as expected from wobble pairing.[25] In the modified duplexes (rF, rL, and 2,3-rL) the thermal stability dropped compared with the A–U paired case, reflecting the loss hydrogen bonding groups at position 7. Among the modified duplexes, the four cases modified with 2,3-rL showed similar thermal stabilities (63–64 °C), but the duplexes modified with rF and rL showed some differences, giving a weak preference for pairing opposite A and G. This small difference in stability could be due to nucleobase stacking stabilization, since purine nucleobases contribute more than pyrimidines.[26] Similar effects have been seen in DNA with dihalogenated deoxyribosides,[27] and Egli and co-workers have reported analogous behavior in RNA utilizing the related 2,4-difluorotoluene analogue.[28] In summary, the steric differen-

ces in the halogenated compounds yielded only small changes in selectivity in the absence of the biological RISC complex.

Shape effects on RNAi activity: For the RNAi experiments at this initial target site we employed a commercial wild-type *Renilla* luciferase plasmid, and to evaluate sequence selectivity, three mutant targets were generated by site-directed mutagenesis of the plasmid. These mutants encode luciferase mRNA with C, G, and U mutations at the position corresponding to position 13 of the passenger RNA (and positioned to be paired opposite position 7 of the modified guide RNAs). The mutations are genetically silent in the *Renilla* luciferase mRNA, as they occur in the third position of the gly171 codon. Thus the reporter protein is unchanged.

We carried out the RNAi experiments employing the wild-type and mutated plasmids to express the desired RNAs in HeLa cells. The results, showing *Renilla* luciferase activity normalized to nontargeted firefly luciferase, are represented in Figure 3. The wild-type guide strand (U at position 7) showed the highest activity when no mismatches were present in the target (WT, with A at the target position). When G and U mutants were targeted, the inhibition of the gene was also strong, as observed previously.[20] Of the three mismatches, only a U:C mismatch at position 7 showed a significant decrease of RNAi activity (C mutant). This relatively low sequence specificity for single mismatches has been observed earlier in a broad study of mutant RNA targets.[29]

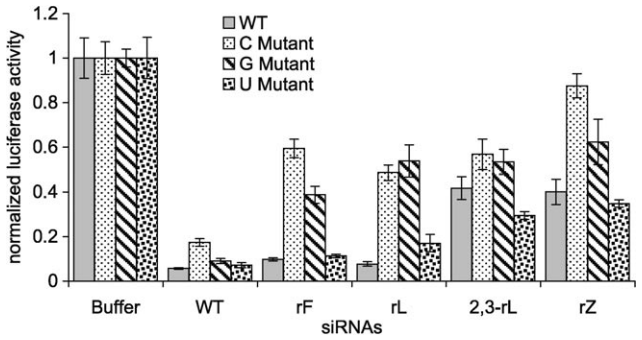

Figure 3. Luciferase suppression activity of natural (WT) and modified (rF, rL, 2,3-rL, rZ) siRNAs at position 7 of the guide strands for singly mismatched mRNA targets. Data were normalized by internal control of a noncomplementary firefly luciferase gene. Data are for the 21 ng RNA amount and are the average of three replicates; error bars reflect standard deviations.

Importantly, two of the modified siRNAs displayed activity nearly the same as the natural siRNA, and most showed sequence selectivity that was better than the wild-type RNA. The siRNAs modified with rF and rL showed strong gene suppression activity against the wild-type *Renilla* luciferase mRNA despite the absence of hydrogen-bonding stabilization at this position. In contrast, the analogues 2,3-rL and rZ showed relatively poor activity. We explain these contrasting effects by the varying shapes of the modified nucleobases. The two highly active analogues retain the shape of uracil, and are thus complementary in shape to the adenine target. However, the poorly active ones do not have the shape of uracil: 2,3-rL has a steric projection (chlorine) at position 7, which is expected to clash sterically with adenine. Analogue rZ is a nucleobase analogue shaped similarly to adenine, and thus would also clash with an adenine partner. Interestingly, a subtle change in size (from rF to rL, which represents a 0.3 Å increase in bond lengths at the halogens) had no strong effect on activity.

The changes in nucleobase shapes at position 7 had substantial effects on sequence selectivity of gene suppression. The two uracil-shaped analogues (rF and rL) showed a similar selectivity profile as U, but with greater selectivity against mismatches. Both analogues showed a preference for the A target, with a secondary preference for a U mismatch, thus behaving similarly to natural uracil. However, both showed a strong selectivity against activity at the G and C mismatches, while the uracil-containing RNA showed only moderate selectivity against C. Thus the two analogues displayed greater sequence selectivity than the natural base. We tentatively attribute the selectivity of the analogues as reflecting a similar shape selectivity of the natural base, but with the addition of stronger destabilization against the most polar partners (C and G), due to the cost of desolvation. We note that this selectivity profile in RNAi activity is markedly different from the pairing selectivity of the RNAs alone (Figure 2). This suggests a pronounced role of the RISC-associated protein(s) in enforcing steric effects that appear to be modest with the RNAs alone. Moreover, it appears that the RISC complex reduces the importance of hydrogen bonding at position 7 that strongly affects the RNAs in the absence of protein.

The nucleobase shape differences also had a substantial effect on the selectivity of the analogues that were not shaped like uracil. Significantly, both of these analogues showed a preference for activity when paired opposite uracil in the target gene, thus reversing the selectivity of the uracil-shaped analogues, which preferred adenine. For the analogue rZ, this can be explained by its steric resemblance to adenine, thus being complementary to uracil in forming a Watson–Crick base-pair shape. Even more interesting is 2,3-rL, which also preferred uracil as a partner in the RISC complex, and showed large differences in activity with different partners even though on its own it shows essentially no pairing selectivity (see Figure 2). A simple steric comparison of 2,3-rL with the four natural nucleobases shows that it most resembles adenine in size and steric projection toward the opposite strand (see Supporting Information). Also significant is the fact that a close analogue of 2,3-rL is paired selectively with thymine by polymerases.[30] Thus the selectivity of analogues rZ and 2,3-rL in cellular RNA interference can also be explained by steric effects that are enforced inside the RISC protein-RNA complex.

Evaluating target generality of size and shape effects: The preceding results provide evidence that the protein/guide RNA/mRNA complex enhances steric effects in RNA–RNA recognition and lowers the importance of hydrogen-bonding-dependent stabilization at some positions. However, these effects were only observed at a single site in an mRNA target. Since RNA forms varied secondary and tertiary structure in different sequence contexts, one may well ask whether such effects would be general (i.e., arising chiefly from the generic RISC structure) or variable with each new RNA target.

To begin to test this we evaluated hydrogen bonding and steric effects at a second target sequence in the *Renilla* luciferase gene, employing the rF and rZ nucleoside analogues as probes in the guide and passenger strands. The siRNAs in this case targeted the site 690–708 of the luciferase gene, 189 nucleotides distant from the previous target (see Figure 4). We substituted uracil residues of the siRNA with rF, and adenine monomers with rZ; in all, ten of the nineteen guide-strand pairing positions were replaced in separate experiments, and two passenger-strand bases were also replaced.

Passenger 3'-TTUUAAACAUGUUGCAGUCCA-5'
Guide 5'-AAUUUGUACAACGUCAGGUTT-3'

Figure 4. Wild-type siRNA duplex targeted to the 690–708 segment of the *Renilla* luciferase gene.

First we measured the effects of single nonpolar analogue substitutions on thermal stability of the siRNA duplex. The results are given in Figure 5. The data show that nonpolar modification at inner positions of the duplex resulted in lower thermal stability, while modifications near the ends had only small effects. This is essentially the same as was observed for the 501–519 target site, as probed with rF in the previous report.[20] The destabilization near the center was similar to that of a mismatch (entry 7A in Figure 5). Similar position-dependent destabilizations were seen for rF and rZ substitutions in the passenger strand as well. Overall, the strongest destabilizations were seen at positions 7–16, while positions 1–4 and 19 were little affected.

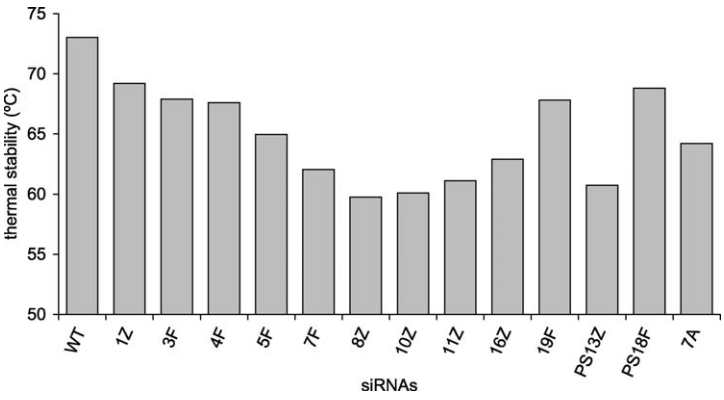

Figure 5. Thermal stability of modified siRNA duplexes targeted to the *Renilla* luciferase 690–708 site. Modifications at the guide strand are denoted with the position number and the modification. F stands for the rF, Z for rZ and A for adenosine. Modifications at the passenger strand are denoted as PS. WT = wild-type.

The RNAi activity of the modified siRNAs in this second context was evaluated targeting the luciferase gene in HeLa cells as before. This provides a test of the importance of hydrogen-bonded stabilization at ten positions along the siRNA duplex in this new sequence context. The results are shown in Figure 6. The duplexes modified on the guide strand at position 1 and 19 with rZ and rF, respectively, showed a gene inhibition activity close to wild-type siRNA (WT). The modified duplexes substituted at positions 3–7 presented moderate activity, while the duplexes substituted at positions 8–16 had no activity in suppressing the luciferase gene. A comparison with the duplex stabilities (Figure 5) shows a general correlation of higher stability with greater RNAi activity. However, position 7 is anomalous, showing stronger activity than expected from its thermal stability. These results are in agreement with our previously reported findings, that is, the nonpolar isostere modifications at the end of the duplexes do not affect the RNAi activity, but near the middle of the strand have significant negative effect. Moreover, the new data are also in agreement with our earlier observation that the position 7 substitution shows higher-than-expected activity despite its inner position in the guide strand and its low thermal stability. This position 7 effect was also observed by Manoharan at an entirely different gene target;[21] thus we believe it to be general to the human RISC complex at many if not all mRNA targets.

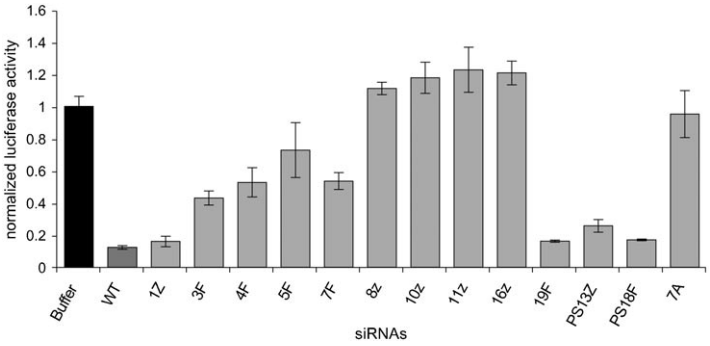

Figure 6. Gene suppression activity of modified siRNAs. Modifications at the guide strand are denoted with the position number and the modification. Modifications at the passenger strand are denoted as PS. Data were normalized by internal control of a noncomplementary firefly luciferase gene. Data are for the 21 ng RNA amount and are the average of three replicates ± standard deviation. WT = wild-type.

The mismatched siRNA 7A has an adenosine at position 7 of the guide strand and shows very low RNAi activity despite its moderate thermal stability. The activity is substantially lower than the 7F nonpolar uracil analogue case. This result further underscores the importance of steric effects at

that position, as the adenine–adenine mismatch may not fit as well as the difluorobenzene–adenine pair inside the active RISC complex.

Modifications to nucleobases might have indirect effects on biological activity of siRNAs; for example, they may stabilize the siRNA duplex against degradation, or enhance its entry into the RISC complex. However, our data suggest that is not the case for the rF and rZ substitutions. The siRNA PS13Z has an rZ modification at position 13 of the passenger strand, pairing it opposite natural rU at position 7 of the guide strand. This duplex has a thermal stability similar to the 7F duplex, but the RNAi activity is close to wild-type. This result supports the idea that the RNAi activity shown by the siRNA 7F is only due to the interaction of the guide strand inside the RISC complex with the messenger RNA.

Finally, we carried out selectivity studies at position 7, employing the wild-type and rF-modified siRNAs. This allowed a second test of whether the selectivity of uracil arises from its hydrogen-bonding ability or its shape. Once again we prepared plasmids encoding three mutated target mRNAs at the complementary position. Similarly to the previous target, the nucleotide required for mutation in the *Renilla* luciferase mRNA is the third one of the val234 codon, which is universally variable without changing the composition of the *Renilla* luciferase protein.

Figure 7 shows the results of the selectivity experiments. As expected, the unmodified siRNA (wt) showed strongest activity against the complementary target mRNA. The U:C and U:G mismatches at position 7 were less well tolerated than the corresponding U:U mismatch, showing a selectivity profile quite similar to that in the previous target site (Figure 3). In the case of the modified siRNA (rF) the selectivity pattern was the same as the wt siRNA, but with decreased activity. The best activity was achieved against the wild-type mRNA and conversely, the C and G mutants showed the lowest RNAi activity. Finally, as in previous examples, the rF:U mismatch was again the best tolerated. Thus in this second target site, the selectivity of a natural nucleobase is well mimicked by an analogue that copies its shape accurately.

Our data at position 7 show that steric effects may be largely if not entirely responsible for base selectivity of the RISC complex. Moreover, some of the analogues yield improved selectivity over natural nucleobases, which may be useful in practical application for avoiding "off-target" effects. In the future it would be of interest to determine steric versus hydrogen-bonding contributions to selectivity at other positions in the complex. Although nonpolar analogues are not well tolerated at some of the other central positions, work is underway to develop new compounds that may be able to contribute information about these other positions.

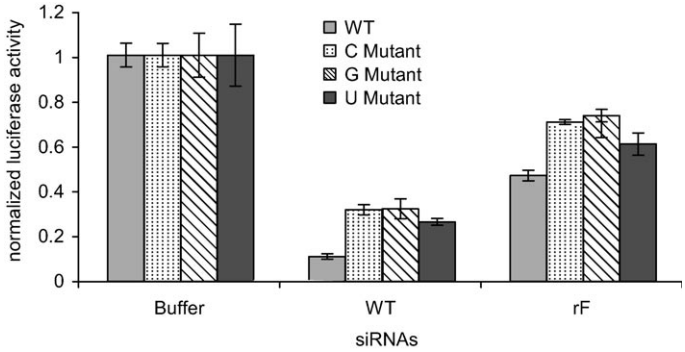

Figure 7. RNAi activity of natural ("WT") and modified ("rF") siRNAs at position 7 of the guide strands for singly mismatched RNA targets. The mismatch is opposite position 7 of the guide strand and involves mutating the corresponding nucleotide in the complementary RNA. Data were normalized by internal control of a noncomplementary firefly luciferase gene. Data are for the 21 ng RNA amount and are the average of three replicates ± standard deviation. WT = wild-type.

Conclusion

A set of nonpolar ribonucleotides, of varied shapes and sizes, has been incorporated into synthetic RNAs for RNAi experiments. The results have shown that hydrogen-bonding stabilization is most important generally at positions 10–16 of the guide RNA, but that hydrogen-bonding deficient nucleobases are well tolerated at positions 1–4, 7, and 19. We find that RNAi activity generally correlates with thermal stability of these substitutions. However, position 7 substitution shows good activity at multiple targets despite its low thermal stability. Further experiments at this position with mutant target mRNAs have pointed out the importance of steric effects on selectivity. Wild-type selectivity for adenine can be achieved or improved utilizing nonpolar nucleosides of similar size and shape to rU, and selectivity for uracil can be evinced by nonpolar adenine shape mimics. Such analogues may be generally useful both as tools for evaluating electrostatic and steric effects in RNA biology.

Experimental Section

General experimental methods: Reagents were purchased from Aldrich and used without further purification. All water-sensitive reactions were carried out in oven-dried glassware with a stirring bar under argon atmosphere. Pyridine and CH_2Cl_2 were dried using a Solvent Purification System (Innovative Technology, USA). All other anhydrous solvents were used directly without further distillation. Thin-layer chromatography was carried out by using Silica Gel 60 F_{254} plates. Column chromatography was performed with Silica Gel (60 Å, 230×400 mesh). All NMR spectra were recorded on 400 or 500 MHz instruments as solutions in the deuterated solvent indicated, and the chemical shifts are reported in ppm. Coupling constants are reported in Hz.

Synthesis of *C*-aryl substituted ribonucleosides (Procedure A): *n*BuLi (1,6 M in hexanes, 3 equiv) was added dropwise to a solution of the corresponding bromo benzene derivative (3 equiv) in Et_2O (0.2 M) at −78 °C under Ar atmosphere. After 30 min a solution of ribonolactone in Et_2O (0.2 M) was added and the resulting solution was stirred for 2 h at −78 °C. The mixture was quenched by addition of NH_4Cl solution, extracted with AcOEt, washed with brine, and dried over $MgSO_4$. The evaporation of the organic solvent afforded a yellowish oil that was used in the next

step. It was dissolved in CH_2Cl_2 (0.2 M) and cooled at −78 °C, then Et_3SiH (3 equiv) and BF_3OEt_2 (3 equiv) were added. The mixture was stirred for 12 h at the same temperature and quenched with a saturated solution of $NaHCO_3$. The aqueous layer was extracted with CH_2Cl_2, and the organic fractions were combined and dried over $MgSO_4$. The residue obtained after evaporation of the solvent was purified by silica chromatography (hexanes/AcOEt 4:1).

2′,3′,5′-Tri-*O*-benzyl-1′-deoxy-β-1′-(2,4-difluorophenyl)-D-ribofuranose (2):[31] Compound **2** was obtained as a white solid in 69% yield by following Procedure A. ^{1}H NMR (400 MHz, $CDCl_3$): δ = 7.61 (dd, J = 15.2, 8.5 Hz, 1H), 7.40–7.27 (m, 15H), 6.79 (dd, J = 8.8, 2.4 Hz 1H), 6.70 (dt, J = 8.4, 2.4 Hz, 1H), 5.39 (d, J = 3.8 Hz, 1H), 4.71 and 4.47 (AB system, J = 12.2 Hz, 2H), 4.65–4.55 (m, 4H), 4.39 (td, J = 6.6, 3.3 Hz, 1H), 4.07 (dd, J = 6.5, 5.0 Hz, 1H), 3.96 (t, J = 4.4 Hz, 1H), 3.86 (dd, J = 10.7, 3.1 Hz, 1H), 3.70 ppm (dd, J = 10.7, 3.5 Hz, 1H).

2′,3′,5′-Tri-*O*-benzyl-1′-deoxy-β-1′-(2,3-dichlorophenyl)-D-ribofuranose (3): Compound **3** was obtained as a white solid in 41% yield by following Procedure A. ^{1}H NMR (400 MHz, $CDCl_3$): δ = 7.74 (dd, J = 7.9, 1.5 Hz, 1H), 7.36–7.26 (m, 16H), 6.97 (t, J = 7.9 Hz, 1H), 5.49 (d, J = 2.5 Hz, 1H), 4.76 (AB system, J = 11.8 Hz, 2H), 4.62 (d, J = 11.8 Hz, 1H), 4.56 (dd, J = 13.5, 11.8 Hz, 2H), 4.42 (d, J = 11.8, 1H), 4.39 (dt, J = 7.9, 2.8 Hz, 2H), 4.08 (dd, J = 7.9, 4.4 Hz, 1H), 3.95 (ddd, J = 13.3, 7.6, 2.5 Hz, 2H), 3.72 ppm (dd, J = 10.8, 3.2 Hz, 1H). ^{13}C NMR (126 MHz, $CDCl_3$): δ = 140.6, 138.2, 138.0, 137.7, 132.7, 129.4, 128.34, 128.33, 128.30, 127.83, 127.78, 127.73, 127.67, 127.60, 127.58, 127.3, 126.5, 81.8, 81.5, 80.0, 77.2, 73.3, 72.4, 72.3, 68.9 ppm. HRMS: m/z calcd for $C_{26}H_{26}NaO_5$ $[M+Na]^+$: 571.1413; found: 571.1435.

2′,3′,5′-Tri-*O*-benzyl-1′-deoxy-β-1′-(2,4-dichlorophenyl)-D-ribofuranose (4): Compound **4** was obtained as a white solid in 58% yield by following Procedure A. ^{1}H NMR (500 MHz, $CDCl_3$): δ = 7.72 (dd, J = 8.5, 0.4 Hz, 1H; ArH), 7.27–7.37 (m, 18H; ArH), 6.99 (ddd, J = 5.8, 2.1 Hz, 0.5, 1H; ArH), 5.44 (d, J = 3.0 Hz, 1H; H1′), 4.72 (dd, J = 24.2, 11.9 Hz, 2H; CH_2OPh), 4.57 (dd, J = 37.8, 11.7 Hz, 2H; CH_2OPh), 4.50 (dd, J = 71.9, 11.9 Hz, 2H; CH_2OPh), 4.36 (dt, J = 7.5, 2.8 Hz, 1H; H4′), 4.03 (dd, J = 7.5, 4.6 Hz, 1H; H3′), 3.88–3.92 (m, 2H; H2′, H5′a), 3.70 ppm (dd, J = 10.8, 3.7 Hz, 1H; H5′b); ^{13}C NMR (126 MHz, $CDCl_3$): δ = 133.8, 132.5, 130.5, 129.6, 129.0, 128.55, 128.52, 128.47, 128.44, 128.39, 127.9, 127.88, 127.85, 127.77, 127.69, 127.35, 127.32, 81.9, 80.6, 80.2, 77.7, 73.4, 72.4, 72.3, 69.1 ppm; HRMS: m/z calcd for $C_{26}H_{26}NaO_5$ $[M+Na]^+$: 571.1413; found: 571.1422.

Removal of the benzyl protecting groups (Procedure B): BBr_3 was added (1 M in dichloromethane, 3.5 equiv) to a solution of tribenzylated nucleoside in dichloromethane (0.1 M) at −78 °C. The mixture was stirred for 3 h, then quenched with methanol at −78 °C and allowed to reach room temperature. After concentration in vacuo, the resulting oil was purified by silica column chromatography (CH_2Cl_2/MeOH 20:1).

1′-Deoxy-β-1′-(2,4-difluorophenyl)-D-ribofuranose (rF nucleoside; 5): Compound **5** was obtained as a white solid in 74% yield by following Procedure B. ^{1}H NMR (400 MHz, $CDCl_3$): δ = 7.72 (dd, J = 15.3, 8.2 Hz, 1H), 6.98 (t, J = 8.8 Hz, 2H), 4.98 (d, J = 5.8 Hz, 1H), 4.28 (AB system, 1H), 4.13 (dd, J = 10.2, 5.1 Hz, 1H), 4.01 (td, J = 11.3, 5.7 Hz, 1H), 3.94 (dd, J = 8.3, 4.1 Hz, 1H), 3.85–3.70 ppm (m, 2H).

1′-Deoxy-β-1′-(2,3-dichlorophenyl)-D-ribofuranose (2,3-rL nucleoside; 6): Compound **6** was obtained as a white solid in 63% yield by following Procedure B. ^{1}H NMR (400 MHz, $CDCl_3$): δ = 7.70 (dd, J = 7.8, 1.0 Hz, 1H), 7.52 (dd, J = 7.9, 1.4 Hz, 1H), 7.35 ppm (t, J = 7.9 Hz, 1H); ^{13}C RMN (101 MHz, $CDCl_3$): δ = 141.3, 132.7, 130.4, 130.0, 128.4, 126.9, 87.3, 85.7, 83.1, 81.7, 62.1 ppm; HRMS: m/z calcd for $C_{11}H_{12}Cl_2NaO_4$ $[M+Na]^+$: 301.0011; found: 301.0014.

1′-Deoxy-β-1′-(2,4-dichlorophenyl)-D-ribofuranose (rL nucleoside; 7): Compound **7** was obtained as a white solid in 56% yield by following Procedure B. ^{1}H NMR (500 MHz, CD_3OD): δ = 7.74 (d, J = 8.5 Hz, 1H; H3), 7.44 (d, J = 2.1 Hz, 1H; H5), 7.32 (dd, J = 8.4, 2.0 Hz, 1H; H6), 5.18 (d, J = 3.9 Hz, 1H; H1′), 3.93–3.98 (m, 2H; H3′, H4′), 3.88–3.91 (m, 1H; H5′a), 3.75–3.78 ppm (m,1H; H5′b); ^{13}C NMR (126 MHz, CD_3OD): δ = 138.9, 134.9, 134.3, 130.8, 129.9, 128.5, 97.0, 85.2, 82.9, 79.0, 71.8, 62.8 ppm; HRMS: m/z calcd for $C_{11}H_{12}Cl_2NaO_4$ $[M+Na]^+$: 301.0005; found: 301.0006.

DMT and TOM protection of nucleosides (Procedure C): The corresponding nucleoside was co-evaporated with anhydrous pyridine (2×) then dissolved in anhydrous pyridine (0.1 M). Diisopropylethylamine (2 equiv) and 4,4′-dimethoxytrityl chloride (DMT-CL; 2 equiv) were added and the mixture was stirred for 4 h at room temperature. The reaction was quenched with methanol and concentrated in vacuo to yield a yellow oil, which was eluted down a short silica gel column (pretreated with 2% NEt_3, run with CH_2Cl_2 then 20:1 CH_2Cl_2/MeOH) to remove the excess of DMT-Cl. The crude 5′-*O*-DMT-protected material was dissolved in 1,2-dichloroethane (0.26 M) and diisopropylethylamine (3.5 equiv) and Bu_2SnCl_2 (1.1 equiv) were added. The reaction was stirred under Ar at room temperature for 1 h, then at 85 °C for 20 min. (Triisopropylsiloxy)methyl chloride (TOMCl; 1.3 equiv) was added. After 20 min at the same temperature, the reaction was quenched by addition of 5% $NaHCO_3$ and cooled to room temperature. The mixture was stirred for 1 h and then extracted with dichloromethane. The organic layers were dried over $MgSO_4$, filtered, and concentrated in vacuo. The residue was purified by column chromatography (silica gel pretreated with 2% NEt_3, hexanes/ethyl acetate 20:1→10:1). The faster eluting 2′-TOM isomers were isolated as foams.

1′-Deoxy-β-1′-(2,4-difluorophenyl)-5-*O*-(4,4′-dimethoxytrityl)-2′-*O*-{[(triisopropylsilyl)oxy]methyl}-D-ribofuranose (9): The isolation of this derivative was more easily achieved by using the additional manipulations explained below. ^{1}H NMR (400 MHz, $CDCl_3$): δ = 7.64 (q, J = 8.4 Hz, 1H), 7.50 (d, J = 7.1 Hz, 2H), 7.39 (dd, J = 8.9, 1.3 Hz, 4H), 7.28 (t, J = 7.1 Hz, 2H), 7.21 (tt, J = 7.3, 1.2 Hz, 1H), 6.82 (d, J = 8.9 Hz, 4H), 6.79 (q, J = 8.5 Hz, 2H), 5.23 (d, J = 5.3 Hz, 1H; C1-H,), 5.04 (AB system, J = 4.7 Hz, 2H; O-CH_2-O), 4.28 (q, J = 5.1 Hz, 1H; C4-H), 4.15 (m, 1H; C3-H)), 4.11 (t, J = 5.3 Hz, 1H; C2-H), 3.79 (s, 6H; $2CH_3O$), 3.48 (dd, J = 10.3 and 2.9 Hz, 1H), 3.35 (dd, J = 10.3, 4.2 Hz, 1H), 3.14 (d, J = 4.8 Hz, 1H; OH), 1.07–1.03 ppm (m, 21H; Si(iPr)$_3$); ^{13}C NMR (101 MHz, $CDCl_3$): δ = 162.5 (dd, J = 227.4, 11.9 Hz), 160.0 (dd, J = 228.8, 11.9 Hz), 158.3 (2C), 144.8, 136.0, 135.9, 130.0 (4C), 129.2 (dd, J = 9.6, 5.7 Hz), 128.2 (2C), 127.7 (2C), 126.7, 123.2 (dd, J = 12.9, 3.6 Hz), 113.0 (4C), 111.2 (dd, J = 21.0, 3.5 Hz), 103.6 (t, J = 25.4 Hz), 90.5, 86.1, 85.3, 83.2, 71.1, 63.5, 55.1 (2C), 46.1, 17.7 (6), 11.7 ppm (3C); ^{19}F NMR (376 MHz, CDCl3): −111.93 (td, J = 15.1, 7.3 Hz), −114.87 ppm (16.9, 8.4 Hz); HRMS (MALDI): m/z calcd for $C_{42}H_{52}O_7F_2NaSi$ $[M+Na^+]$: 757.3343; found: 757.3307.

1′-Deoxy-β-1′-(2,3-dichlorophenyl)-5-*O*-(4,4′-dimethoxytrityl)-2′-*O*-{[(triisopropylsilyl)oxy]methyl}-D-ribofuranose (10): Compound **10** was obtained as a white foam in 33% yield by following Procedure C. ^{1}H NMR (400 MHz, $CDCl_3$): δ = 7.80 (d, J = 7.8 Hz, 1H), 7.52 (d, J = 7.1 Hz, 2H), 7.41 (d, J = 8.9 Hz, 4H), 7.40–7.36 (m, 1H) 7.29 (t, J = 7.1 Hz, 2H), 7.22 (t, J = 7.2 Hz, 1H), 7.06 (t, J = 7.9 Hz, 1H), 6.83 (d, J = 8.9 Hz, 4H), 5.43 (d, J = 2.9 Hz, 1H), 5.26 (d, J = 4.8 Hz, 1H), 4.98 (d, J = 4.9 Hz, 1H), 4.25–4.18 (m, 1H), 4.17–4.12 (m, 1H), 4.10–4.06 (m, 1H), 3.79 (s, 6H), 3.49 (ddd , J = 14.8, 10.5, 3.3 Hz, 2.), 3.48 (d, J = 6.6 Hz, 1H), 1.06 ppm (s, 21H); ^{13}C RMN (101 MHz, $CDCl_3$): δ = 158.4 (2C), 144.9, 140.5, 136.1, 135.9, 132.8, 130.2 (4C), 130.1, 129.4, 128.3 (2C), 127.8 (2C), 127.5, 126.7, 126.3, 113.1 (4C), 90.8, 86.6, 86.2, 82.4, 81.4, 70.1, 63.1, 55.2 (2C), 17.8 (4C), 17.7 (2C), 12.2, 11.8 ppm (2C); HRMS: m/z calcd for $C_{42}H_{52}Cl_2O_7NaSi$ $[M+Na]^+$: 789.2757; found: 789.2747.

1′-Deoxy-β-1′-(2,4-dichlorophenyl)-5-*O*-(4,4′-dimethoxytrityl)-2′-*O*-{[(triisopropylsilyl)oxy]methyl}-D-ribofuranose (11): Compound **11** was obtained as a white foam in 43% yield by following Procedure C. ^{1}H NMR (500 MHz, $CDCl_3$): δ = 7.79 (d, J = 8.5 Hz, 1H; ArH), 7.52 (d, J = 7.3 Hz, 1H; ArH), 7.39–7.42 (m, 5H; ArH), 7.29–7.32 (m, 3H; ArH), 7.25 (t, J = 7.3 Hz, 1H; ArH), 7.10 (dd, J = 8.5, 2.0 Hz, 1H; ArH), 6.85 (d, J = 8.8 Hz, 4H; ArH), 5.37 (d, J = 3.4 Hz, 1H; H1′), 5.11 (dd, J = 134, 4.8 Hz, 2H; CH_2OSi), 4.24 (app dd, J = 11.9, 6.5 Hz, 1H; H4′), 4.13–4.16 (m, 1H; H3′), 4.08 (app t, J = 4.1 Hz, 1H; H2′), 3.82 (s, 6H; OCH_3), 3.54 (dd, J = 10.5, 2.3 Hz, 1H; H5′a), 3.42 (dd, J = 10.5, 4.3 Hz, 1H; H5′b), 3.40 (d, J = 3.4 Hz, 1H; 3′-OH), 1.06–1.15 ppm (m, 21H; $3CH(CH_3)_2$); ^{13}C NMR (126 MHz, $CDCl_3$): δ = 158.7, 136.9, 136.2, 136.0, 133.9, 132.8, 130.4, 130.31, 130.27, 129.3, 129.1, 128.4, 127.9, 127.4, 126.8, 113.2, 90.8, 86.6, 82.8, 80.4, 70.5, 63.2, 55.1, 17.9, 11.9 ppm; HRMS: m/z calcd for $C_{42}H_{52}Cl_2O_7NaSi$$[M+Na]^+$: 789.2752; found: 789.2743.

Procedure for 2′-*O*-TOM-rF purification: The crude product from the TOM protection reaction was dissolved in dichloromethane (0.2 M), and diisopropylethylamine (4 equiv), Ac_2O (2 equiv) and DMAP (cat) were added at 0 °C. After 15 min the mixture was allowed to reach room temperature and stirred for 2 h. The reaction was quenched with $NaHCO_3$, extracted with CH_2Cl_2, dried over $MgSO_4$, and concentrated. Alter flash chromatography purification (hexanes/EtOAc 12:1), the 2′- and 3′-TOM-protected isomers were isolated in 51 and 28% yield, respectively.

3′-*O*-Acetyl-1-deoxy-1-(2,4-difluorophenyl)-5′-*O*-(4,4′-dimethoxytrityl)-2′-*O*-{[(triisopropylsilyl)oxy]methyl}-β-D-ribofuranose: ^{1}H NMR (400 MHz, $CDCl_3$): δ = 7.68 (q, J = 14.7, 8.0 Hz, 1H), 7.54 (d, J = 7.3 Hz, 2H), 7.43 (dd, J = 8.6, 1.6 Hz, 4H), 7.32 (t, J = 7.7 Hz, 2H), 7.25 (t, J = 7.4 Hz, 1H), 6.87 (d, J = 8.8 Hz,4H), 6.90–6.80 (m, 2H), 5.40 (dd, J = 5.0, 4.0 Hz, 1H), 5.27 (d, J = 7.2 Hz, 1H), 4.93 (s, 2H), 4.54 (dd, J = 7.1, 5.4 Hz, 1H), 4.30 (q, J = 3.5 Hz, 1H), 3.79 (s, 6H), 3.54 (dd, J = 10.4, 3.3 Hz, 1H), 3.41 (dd, J = 10.4, 3.7 Hz, 1H), 2.14 (s, 3H), 1.01 ppm (s, 21H); ^{13}C NMR (100 MHz, $CDCl_3$): δ = 170.1 (C=O), 162.9 (C–F, dd, J = 182.9, 12.0 Hz), 160.4 (C–F, dd, J = 184.5, 11.9 Hz), 158.4 (2C, C–OMe), 144.6, 135.8, 135.7, 130.0 (2C), 129.9 (2C), 129.5 (dd, J = 9.7, 5.2 Hz), 128.1 (2C), 127.7 (2C), 126.7, 122.3 (dd, J = 12.7, 3.7 Hz) 113.0 (4C), 111.2 (dd, J = 20.9, 3.4 Hz), 103.5 (t, J = 25.6 Hz), 88.9, 86.3, 81.8, 79.4, 76.0, 75.9, 72.4, 63.2, 54.9 (2C), 20.8, 17.6 (6C), 11.6 ppm (3C); 19F NMR (376 MHz, $CDCl_3$): −111.74 (td, J = 15.6, 8.0 Hz), −114.65 ppm (dd, J = 15.6, 7.9 Hz); HRMS (MALDI +): m/z calcd for $C_{44}H_{54}O_8F_2NaSi$ [M+Na$^+$]: 799.3448; found: 799.3461.

2′-*O*-Acetyl-1-deoxy-1-(2,4-difluorophenyl)-5′-*O*-(4,4′-dimethoxytrityl)-3′-*O*-{[(triisopropylsilyl)oxy] methyl}-β-D-ribofuranose: ^{1}H NMR (400 MHz, $CDCl_3$): δ = 7.57 (dd, J = 15.5, 7.5 Hz, 1H), 7.50 (d, J = 8.0 Hz, 2H), 7.38 (d, J = 8.8 Hz, 4H), 7.28 (t, J = 8.0 Hz, 2H), 7.21 (t, J = 7.5 H; 1H), 6.82 (d, J = 8.8 Hz, 4H), 6.81–6.35 (m, 2H), 5.29 (d, J = 5.4 Hz, 1H), 5.21 (t, J = 5.4 Hz, 1H), 4.89 (d, J = 4.8 Hz, 1H), 4.76 (d, J = 4.8 Hz, 1H), 4.42–4.37 (m, 1H), 4.36–4.32 (m, 1H), 3.79 (s, 6H), 3.54 (d, J = 10.7 Hz, 1H), 3.35 (dd, J = 10.4, 4.8 Hz, 1H), 2.12 (s, 3H), 1.15 (s, 3H), 0.96 ppm (s, 18H); ^{13}C NMR (100 MHz, $CDCl_3$): δ = 169.9, 162.6 (dd, J = 238.3, 11.8 Hz), 160.2 (dd, J = 240.4, 12.1 Hz), 158.4 (2C), 144.7, 135.9, 135.8, 130.2 (4C), 128.9 (dd, J = 10.7, 6.7 Hz), 128.3 (2C), 127.7 (2C), 126.7, 122.5 (dd, J = 13.1, 3.7 Hz), 113.0 (4C), 111.3 (dd, J = 20.9, 3.5 Hz), 103.7 (t, J = 25.4 Hz), 89.4, 86.2, 81.9, 76.6, 76.3, 74.7, 63.4, 54.1 (2C), 20.8, 17.7 (6C), 11.7 ppm (3C); ^{19}F NMR (376 MHz, $CDCl_3$) : −111.54 (td, J = 15.3, 7. 7 Hz), −114.59 (dd, J = 17.6, 8.2 Hz); HRMS (MALDI+): m/z calcd for $C_{44}H_{54}O_8F_2NaSi$ [M+Na]$^+$: 799.3448; found: 799.3450.

The 2′-TOM-protected isomer was dissolved in CH_2Cl_2 (0.6 M) and a solution of NH_3 (in MeOH 7 M) was added to make a 0.04 M solution. The mixture was stirred for 10 h at room temperature, then it was concentrated in vacuo and purified by silica column chromatography (hexanes/EtOAc 10:1) affording the alcohol **9** as a white foam in 86% yield.

Synthesis of phosphoramidites (Procedure D): Diisopropylethylamine (3 equiv) and 2-cyanoethyl-*N*,*N*-diisopropylchlorophosphoramidite (1.5 equiv) were added to a solution of the corresponding 5′-*O*-DMT-2′-*O*-TOM-protected nucleoside in dichloromethane (0.2 M) at 0 °C. The reaction mixture was stirred at room temperature for 3 h, then the mixture was loaded directly onto a silica gel column for purification (hexanes/ethyl acetate 6:1, +2% NEt_3).

1′-Deoxy-β-1′-(2,4-difluorophenyl)-5-*O*-(4,4′-dimethoxytrityl)-2′-*O*-{[tri-isopropylsilyl)oxy]methyl}-D-ribofuranose-3′-*O*-cyanoethyl-*N*,*N*-diisopropylphosphoramidite (13): Compound **13** was obtained as white foam in 91% yield by following Procedure D. ^{1}H NMR (400 MHz, $CDCl_3$): δ = 7.67–7.55 (m, 1H), 7.48 (t, J = 6.9 Hz, 2H), 7.37 (dt, J = 8.9, 1.1 Hz, 4H), 7.31–7.18 (m, 3H), 6.81 (t, J = 8.4 Hz, 4H), 6.78–6.71 (m, 2H), 5.23 (d, J = 6.3 Hz, 1H), 4.96 (d, J = 5.1 Hz, 1H), 4.92 (dd, J = 7.8, 5.9 Hz, 2H), 5.89 (d, J = 5.1 Hz, 1H), 4.37 (ddd, J = 14.1, 4.4, 4.4 Hz, 1H), 4.28 (m, 1H), 3.97–3.80 (m, 1H), 3.78 and 3.77 (2 s, 6H), 3.62–3.47 (m, 2H), 3.44 (dd, J = 10.3, 3.3 Hz, 1H), 3.26 (ddd, J = 10.6, 6.6, 4.3 Hz, 1H), 2.64 (dd, J = 12.6, 6.4 Hz, 1H), 2.30 (t, J = 6.7 Hz, 1H), 1.14 (d, J = 6.7 Hz, 12H), 0.95 ppm (s, 21H); ^{13}C NMR (126 MHz, $CDCl_3$): δ = 163.5, 161.5 and 169.7 (3m), 158.4, 144.8, 144.7, 136.0, 135.9, 135.9, 135.8, 130.2, 130.1, 129.5 (m), 128.4, 128.3, 127.7, 126.8, 126.7, 124.8, 123.2 (dd, J = 12.9, 3.7 Hz), 123.0 (dd, J = 12.9, 3.0 Hz), 117.7, 117.4, 113.0, 111.2 (dd, J = 9.3, 3.0 Hz), 111.0 (dd, J = 9.9, 2.8 Hz), 103.6 (dt, J = 25.5, 5.7 Hz), 90.0, 88.9, 88.7, 86.3, 86.2, 83.2 (m), 80.5, 79.8, 79.7, 76.2, 72.2, 72.1, 71.8, 71.7, 63.6, 63.1, 58.9, 58.8, 57.9, 57.8, 55.2, 55.1, 43.3, 43.2, 43.0, 42.9, 24.5 (m), 20.6, 20.3, 20.2, 20.0, 19.9, 17.7, 11.8 ppm; ^{19}F NMR (376 MHz, $CDCl_3$): δ = −112.19 (td, J = 15.4, 7.7 Hz; major isomer), −114.10 (td, J = 15.6, 7.9 Hz; minor isomer), −114.38 ppm (dd, J = 17.7, 8.0 Hz); ^{31}P NMR (162 MHz, $CDCl_3$): δ = 148.34 (s; major isomer), 148.11 ppm (s; minor isomer); HRMS (MALDI): m/z calcd for $C_{51}H_{69}N_2O_8F_2NaSiP$ [M+Na]$^+$: 957.4421; found: 957.4389.

1′-Deoxy-β-1′-(2,3-dichlorophenyl)-5-*O*-(4,4′-dimethoxytrityl)-2′-*O*-{[tri-isopropylsilyl)oxy]methyl}-D-ribofuranose-3′-*O*-cyanoethyl-*N*,*N*-diisopropylphosphoramidite (14): Compound **14** was obtained as white foam in 70% yield by following Procedure D. ^{1}H NMR (400 MHz, $CDCl_3$): 7.79 and 7.72 (dd, J = 7.8, 1.5 Hz, 1H), 7.49 (t, J = 7.0 Hz, 2H), 7.38 (dt, J = 8.9, 2.4 Hz, 5H), 7.32–7.18 (m, 3H), 7.08–7.00 (m, 1H), 6.82 (t, J = 8.4 Hz, 4H), 5.52–5.59 (m, 1H), 5.05–5.92 (AB systems, 2H), 4.41–4.18 (m, 2H), 3.79 and 3.78 (2 s, 6H), 3.71–3.46 (m, 5H), 3.31 (dt, J = 8.9, 3.9 Hz, 1H), 2.71–2.56 (m, 2H), 2.30 (t, J = 6.7 Hz, 1H), 1.17–1.07 (m, 12H), 0.98 and 0.97 ppm (2 s, 21H); ^{13}C NMR (126 MHz, $CDCl_3$): 158.4, 144.6, 140.4, 140.2, 135.9–135.8, 132.8, 132.8, 131.3, 131.0, 130.2, 130.1, 129.5, 129.4, 128.4, 128.3, 127.8, 127.3, 127.3, 126.8, 126.7, 126.5, 126.4, 117.6, 117.4, 113.0, 89.2, 86.3, 82.7, 81.6, 80.3, 79.7, 71.8, 71.5, 63.2, 62.7, 58.8, 58.7, 57.9, 57.8, 57.2, 56.9, 55.2, 43.3, 42.2, 29.7, 24.5, 20.3, 20.0, 17.7, 12.6, 11.9 ppm; ^{31}P NMR (162 MHz, $CDCl_3$): δ = 150.75 (s; major isomer), 150.58 ppm (s; minor isomer).

1′-Deoxy-β-1′-(2,4-dichlorophenyl)-5-*O*-(4,4′-dimethoxytrityl)-2′-*O*-{[tri-isopropylsilyl)oxy]methyl}-D-ribofuranose-3′-*O*-cyanoethyl-*N*,*N*-diisopropylphosphoramidite (15): Compound **15** was obtained as white foam in 90% yield by following Procedure D. ^{1}H NMR (500 MHz, $CDCl_3$): δ = 7.76 (d, J = 8.4 Hz, 1H; ArH), 7.52–7.46 (m, 2H; ArH), 7.39–7.20 (m, 8H; ArH), 7.09–7.05 (m, 1H; ArH), 6.83 (d, J = 8.9 Hz, 4H; ArH), 5.42 (d, J = 5.16 Hz, 1H; H1′), 5.02–4.92 (m, 2H; OCH_2OSi), 4.40–4.38 (m, 3H; H2′, H3′, H4′), 3.80 (s, 6H; OCH_3), 3.55 (m, 2H; CH_2CN), 2.31 (t, J = 6.62 Hz, 2H; OCH_2), 1.13 (m, 14H; $CH(CH_3)_2$), 0.97 ppm (s, 21H; $SiCH(CH_3)_2$). ^{13}C NMR (100 MHz, $CDCl_3$): δ = 158.6, 149.5, 136.1–133.7, 130.5–126.8, 113.1, 86.5, 80.8, 63.0, 58.2, 55.2, 43.3, 24.7, 17.7, 11.8 ppm; ^{31}P NMR (126 MHz, $CDCl_3$): δ = 150.80, 150.75 ppm; HRMS: m/z calcd for $C_{51}H_{70}N_2O_8SiPCl_2$ [M+H]$^+$: 967.4016; found: 967.4037.

1-[5-*O*-(4,4′-Dimethoxytriphenylmethyl)-β-D-erythropentofuranosyl]-4-methyl-1*H*-benzimidazole: Diisopropylethylamine (1.9 mL, 10.9 mMol) and 4,4′-dimethoxytrityl chloride (3.6 g, 10.6 mMol) were added to a solution of benzimidazole free nucleoside (1.4 g, 5.30 mmol) in pyridine (50 mL) at 0 °C. The mixture was stirred at room temperature for 4 h, then it was quenched with methanol, concentrated in vacuo and purified by silica column chromatography (CH_2Cl_2/MeOH, 20:1; NEt_3 2%) to yield a white foam (50%). ^{1}H NMR (400 MHz, $CDCl_3$): δ = 7.68 (d, J = 2.1 Hz, 1H), 7.50 (d, J = 8.0 Hz, 1H), 7.43 (dd, J = 8.1, 1.3 Hz, 2H), 7.31 (dd, J = 8.9, 2.1 Hz, 4H), 7.25–7.16 (m, 3H), 6.86 (d, J = 7.3 Hz, 1H), 6.81 (d, J = 7.8 Hz, 1H), 6.76 (dd, J = 8.9, 5.5 Hz, 4H), 5.81 (d, J = 6.4 Hz, 1H), 4.72 (t, J = 6.1 Hz, 1H), 4.50 (dd, J = 5.8, 3.1 Hz, 1H), 4.27 (q, J = 3.2 Hz, 1H), 3.76 and 3.75 (2 s, 6H), 3.46 (d, J = 3.3 Hz, 2H), 2.43 ppm (s, 3H); ^{13}C NMR (100 MHz, $CDCl_3$): δ = 158.5 (2C), 144.5, 142.1, 140.6, 135.6, 135.4, 131.7, 130.1 (4C), 129.1, 128.1 (2C), 127.9 (2C), 126.9, 123.5, 123.4, 113.1 (4C), 109.7, 90.1, 86.6, 84.0, 72.8, 71.1, 63.5, 55.2 (2C), 16.6 ppm; HRMS: m/z calcd for $C_{34}H_{35}N_2O_6$ [M+H]$^+$: 567.2495; found: 567.2508.

1-Deoxy-5-*O*-(4,4′-dimethoxytrityl)-1′-(4-methyl-1*H*-benzimidazolyl)-2′-*O*-{[(triisopropylsilyl)oxy]methyl}-β-D-erythropentofuranose (12): Diisopropylethylamine (1 mL, 5.74 mMol) and Bu_2SnCl_2 (550 mg, 1.81 mMol) were added to a solution of the DMT-protected benzimidazole derivative (927 mg, 1.64 mMol) in dichloromethane (6.6 mL). The mixture was stirred at room temperature for 2 h. Then it was heated to 85 °C for 20 min and (Triisopropylsiloxy)methyl chloride (494 μL, 2.13 mMol) was added. The mixture was stirred at the same temperature for 20 min, quenched by addition of 5% $NaHCO_3$ and cooled to room temperature. The mixture was stirred for 1 h, then extracted with dichloromethane. The organic layers were dried over $MgSO_4$, filtered and concentrated in vacuo. The residue was purified by column chromatography (silica gel pretreated with 2% NEt_3, hexanes/ethyl acetate 2:1). The faster eluting

2′-TOM isomer was isolated as foam (9%). ^{1}H NMR (400 MHz, [D$_6$]acetone): δ=8.25 (s, 1H), 7.54 (d, J=6.8 Hz, 1H), 7.49 (d, J=8.2 Hz, 2H), 7.37 (d, J=8.4 Hz, 4H), 7.29 (tt, J=8.3, 1.7 Hz, 2H), 7.22 (tt, J=6.2, 1.3 Hz, 1H), 7.05–6.99 (m, 2H), 6.85 (dd, J=9.0, 1.2 Hz, 4H), 6.13 (d, J=5.9 Hz, 1H), 5.09 (AB system, J=5.2 Hz, 2H), 4.82 (t, J=5.6 Hz, 1H), 4.61 (dd, J=9.3, 4.7 Hz, 1H), 4.27 (q, J=3.8 Hz, 1H), 4.14 (d, J=4.6 Hz, 1H), 3.77 and 3.76 (2 s, 6H), 3.44 (d, J=3.6 Hz, 2H), 2.58 (s, 3H), 1.03–0.95 ppm (m, 21H); ^{13}C NMR (100 MHz, [D$_6$]acetone): δ= 160.6 (2C), 146.9, 145.7, 142.6, 137.6, 137.5, 134.6, 132.0 (2C), 131.9 (2C), 131.6, 129.9 (2C), 129.6 (2C), 128.6, 124.5, 124.2, 114.9 (4C) 110.9, 91.8, 89.6, 88.2, 85.8, 81.6, 71.9, 65.4, 56.4 (2C), 19.1 (6C), 17.7, 13.5 ppm (3C); HRMS: m/z calcd for $C_{44}H_{57}N_2O_7Si$ $[M+H]^+$: 753.3935; found: 753.3941.

1-Deoxy-5-*O*-(4,4′-dimethoxytrityl)-1′-(4-methyl-1*H*-benzimidazolyl)-2′-*O*-{[(triisopropylsilyl)oxy]methyl}-β-D-erythropentofuranose-3′-*O*-cyanoethyl-*N*,*N*-diisopropylphosphoramidite (16): Diisopropylethylamine (82 μL), methylimidazole (9.3 μL) and *N*,*N*-diisopropylchlorophosphoramidite (79 μL) were added to a solution of **12** (108 mg) in CH_2Cl_2 (15 mL) at 0°C. The mixture was stirred for 2 h at room temperature, the solvent was evaporated, and the crude reaction was purified by silica column chromatography (hexanes/AcOEt 2:1, Et_3N 2%). The corresponding phosphoramidite was isolated as a white foam (76%). ^{1}H NMR (400 MHz, $CDCl_3$): δ=8.14 and 8.12 (2 s, 1H), 7.51–7.46 (m, 3H), 7.34 (t, J=8.9 Hz, 4H), 7.30–7.17 (m, 3H), 7.07–6.98 (m, 2H), 6.81 (t, J=8.7 Hz, 4H), 6.09 and 6.05 (d, J=6.0 Hz, 1H), 4.96–4.88 (m, 2H), 4.76 and 4.72 (t, J=5.6 Hz, 1H), 4.58–4.48 (m, 1H), 4.39 and 4.35 (q, J=3.4 Hz, 1H), 3.96–3.80 (m, 2H), 3.78, 3.77, 3.76 and 3.75 (4 s, 6H), 3.66–3.52 (m, 3H), 3.49 and 3.46 (d, J=3.1 Hz, 1H), 3.40–3.44 (m, 1H), 2.66 (s, 3H), 2.65–2.60 (m, 1H), 2.31 (dt, J=6.5, 1.8 Hz, 1H), 1.18 (t, J=6.0, 8H), 1.03 (d, J=6.7 Hz, 4H), 0.92 and 0.89 ppm (2s, 20H); ^{13}C NMR (100 MHz, $CDCl_3$): δ=158.4, 144.4, 144.3, 143.5, 143.4, 140.2, 140.1, 135.6, 135.5, 135.4, 132.4, 132.4, 132.3, 130.1, 130.0, 128.2, 128.1, 127.8, 126.9, 126.8, 123.0, 122.9, 122.8, 122.7, 117.5, 117.2, 113.1, 108.9, 108.7, 89.6, 89.5, 89.2, 89.1, 88.1, 87.9, 86.6, 86.5, 83.7, 83.6, 83.3, 83.3, 78.1, 78.0, 77.3, 77.2, 71.4, 71.3, 71.1, 70.9, 63.2, 62.8, 58.9, 58.7, 57.9, 57.7, 55.1, 43.4, 43.2, 43.1, 43.0, 24.6, 24.5, 24.4, 17.6, 17.5, 16.6, 11.7 ppm; ^{31}P NMR (126 MHz, $CDCl_3$): δ=151.98, 151.35 ppm; HRMS: m/z calcd for $C_{53}H_{74}N_4O_9SiP$ $[M+H+O]^+$ (oxidized): 969.4963; found: 969.4970.

RNA synthesis and purification methods: RNA oligonucleotides were synthesized BY using 2′-TOM phosphoramidites. Acetonitrile (synthesis grade), the standard 2′-TOM phosphoramidites for A, C, G, and U, 5-ethylthio-1*H*-tetrazole, and other standard solutions were obtained from commercial suppliers. RNA oligonucleotides were synthesized on the 1 μmol scale. The standard coupling time of 6 min was used for the four standard phosphoramidites, and an increased coupling time of 10 min was used for the modified phosphoramidites. After the solid-phase synthesis, the solid support was transferred to a screw-cap glass vial and incubated at room temperature for 16 h with 1.5 mL of methylamine solution, prepared by mixing equal volumes of 40% aqueous methylamine and 33% methylamine in ethanol. After the vial was cooled briefly on ice, the supernatant was transferred by pipette into 2 mL Eppendorf tubes; the solid support and vial were rinsed with 50% ethanol (2× 0.25 mL). The combined solutions were evaporated to dryness using an evaporating centrifuge. The residue was dissolved in a total volume of 1.0 mL of TBAF (1 M) in THF and rocked at 37°C for 12 h. Tris·HCl (1 mL, 1 M), pH 7.5, was added to the solution, and the oligonucleotide was desalted on a NAP-10 column by using water as the eluent and evaporated to dryness. The oligonucleotides were purified by 20% denaturing PAGE, isolated by the crush and soak method and quantitated by absorbance at 260 nm. Mutated passenger strands (C, G and U) were synthesized by Integrated DNA Technologies (Coralville, IA).

Thermal denaturation methods: Oligonucleotides (0.5 μM each) were dissolved in buffer (50 mM potassium acetate, 1 mM magnesium acetate, 15 mM HEPES-KOH at pH 7.4). Experiments were performed in Teflon-stoppered 1 cm path length quartz cells on a Varian Cary 1 UV/Vis spectrophotometer equipped with thermoprogrammer. The samples were heated to 90°C, allowed to slowly cool to 25°C, and then warmed during the denaturation experiments at a rate of 1°C min^{-1} to 80°C, monitoring absorbance at 260 nm. In all cases the complexes displayed sharp, apparently two-state transitions. The data were analyzed by the denaturation curve-processing program, MeltWin v. 3.0. Melting temperatures (T_m) were determined by computer-fit of the first derivative of absorbance with respect to 1/T.

Preparation of mutant luciferase plasmid vectors: The luciferase gene in the pRL CMV vector (Promega, Madison, WI) was mutated at position 1580 and 1769 to create three different mutant constructs at both positions that differ from the wild type by single nucleotide substitutions. These substitutions do not create a corresponding change in amino acid residue in the luciferase gene, but retain the same amino acid residue, glycine, as in the wild-type construct. By using three pairs of designed primers (Supplementary), one pair for each mutant (A to T, A to C, and A to G), mutant gene constructs were made with the site-directed mutagenesis kit, (Stratagene, La Jolla, CA) following the protocol provided by the manufacturer. The resulting constructs were sequenced to confirm the required mutations in the gene (Supporting Information).

RNA interference methods: Hela cells were grown at 37°C, 5% CO_2 in Dulbecco's modified Eagles's medium (DMEM, GIBCO) supplemented with 10% fetal bovine serum (FBS), 100 U mL^{-1} penicillin and 100 μg mL^{-1} streptomycin. The cells were maintained in exponential growth. The cells were plated in 24-well plates (0.5 mL medium per well) to reach about 50% confluence at transfection. The cells were grown for 24 h and the culture medium was changed to OPTIMEM 1 (GIBCO), 0.5 mL per well. Two luciferase plasmids, *Renilla* luciferase (pRL-CMV) and firefly luciferase (pGL3) from Promega, were used as reporter and control, respectively. Co-transfection of plasmids and siRNAs was carried out with GeneSilencer (GTS) as described by the manufacturer for adherent cell lines. Per well, 0.17 μg pGL3, 0.017 μg pRL-CMV and 2.1 ng siRNAs, formulated into liposomes, were applied. The final volume was 500 μL per well. The cells were harvested 22 h after transfection, and lysed by using passive lysis buffer (PLB), 100 μL per well, according to the instructions of the Dual-Luciferase Reporter Assay System (Promega, USA). The luciferase activities of the samples were measured using a Fluoroskan Ascent FL Luminometer (Thermo Electron Corporation, USA) with a delay time of 2 s and an integrate time of 10 s. The volumes used were: 20 μL of sample and 30 μL of each reagent (luciferase assay reagent II and Stop & Glo Reagent). The inhibitory effects generated by siRNAs were expressed as normalized ratios between the activities of the reporter (*Renilla*) luciferase gene and the control (firefly) luciferase gene.

Acknowledgements

This work was supported by the US National Institutes of Health (GM072705). A.S. acknowledges support from Marie Curie OIF Fellowship (6th Framework Program, UE). A.P.S. acknowledges support from a National Science Foundation Graduate Fellowship and a Lieberman Fellowship. R.M.M. acknowledges the Bing Program for a fellowship.

[1] a) A. Fire, S. Xu, M. K. Montgomery, S. A. Kostas, S. E. Driver, C. C. Mello, *Nature* **1998**, *391*, 806–811; b) D. Bumcrot, M. Manoharan, V. Koteliansky, D. W. Y. Sah, *Nat. Chem. Biol.* **2006**, *2*, 711–719.

[2] a) S. M. Elbashir, W. Lendeckel, T. Tuschl, *Genes Dev.* **2001**, *15*, 188–200; b) S. M. Elbashir, J. Martinez, A. Patkaniowska, W. Lendeckel, T. Tuschl, *EMBO J.* **2001**, *20*, 6877–6888.

[3] a) J.-Y. Yu, S. L. DeRuiter, D. L. Turner, *Proc. Natl. Acad. Sci. USA* **2002**, *99*, 6047–6052; b) P. J. Paddison, A. A. Caudy, E. Bernstein, G. J. Hannon, D. S. Conklin, *Genes Dev.* **2002**, *16*, 948–958.

[4] F. Czauderna, M. Fechtner, S. Dames, H. Aygün, A. Klippel, G. J. Pronk, K. Giese, J. Kaufmann, *Nucleic Acids Res.* **2003**, *31*, 2705–2716.

[5] M. A. Valencia-Sanchez, J. Liu, G. J. Hannon, R. Parker, *Genes Dev.* **2006**, *20*, 515–524.

[6] a) D. S. Schwarz, G. Hutvágner, T. Du, Z. Xu, N. Aronin, P. D. Zamore, *Cell* **2003**, *115*, 199–208; b) Y. Tomari, C. Matranga, B. Haley, N. Martinez, P. D. Zamore, *Science* **2004**, *306*, 1377–1380; c) G. Hutvagner, *FEBS Lett.* **2005**, *579*, 5850–5857.
[7] a) C. Matranga, Y. Tomari, C. Shin, D. P. Bartel, P. D. Zamore, *Cell* **2005**, *123*, 607–620; b) T. A. Rand, S. Petersen, F. Du, X. Wang, *Cell* **2005**, *123*, 621–629.
[8] G. Meister, M. Landthaler, A. Patkaniwska, Y. Dorsett, G. Teng, T. Tuschl, *Mol. Cell* **2004**, *15*, 185–197.
[9] a) A. L. Jackson, S. R. Bartz, J. Schelter, S. V. Kobayashi, J. Burchad, M. Mao, B. Li, G. Cavet, P. S. Linsley, *Nat. Biotechnol.* **2003**, *21*, 635–637; b) L. M. Alemán, J. Doench, P. A. Sharp, *RNA* **2007**, *13*, 385–395.
[10] J. A. H. Hoerter, N. G. Walter, *RNA* **2007**, *13*, 1887–1893.
[11] C. Wolfrum, S. Shi, K. N. Jayaprakash, M. Jayaraman, G. Wang, R. K. Pandey, K. G. Rajeev, T. Nakayama, K. Charrise, E. M. Ndungo, T. Zimmermann, V. Koteliansky, M. Manoharan, M. Stoffel, *Nat. Biotechnol.* **2007**, *25*, 1149–1157.
[12] a) M. Amarzguioui, T. Holen, E. Babaie, H. Prydz, *Nucleic Acids Res.* **2003**, *31*, 589–595; b) M. Manoharan, *Curr. Opin. Chem. Biol.* **2004**, *8*, 570–579; c) A. L. Jackson, J. Burchard, D. Leake, A. Reynolds, J. Schelter, J. Guo, J. M. Johnson, L. Lim, J. Karpilow, K. Nichols, W. Marshall, A. Khvorova, P. S. Linsley, *RNA* **2006**, *12*, 1197–1205; d) Y. Fedorov, E. M. Anderson, A. Birmingham, A. Reynolds, J. Karpilow, K. Robinson, D. Leake, W. S. Marshall, A. Khvorova, *RNA* **2006**, *12*, 1188–1196.
[13] J. Soutschek, A. Akinc, B. Bramlage, K. Charisse, R. Constien, M. Donoghue, S. Elbashir, A. Geick, P. Hadwiger, J. Harborth, M. John, V. Kesavan, G. Lavine, R. K. Pandey, T. Racie, K. G. Rajeev, I. Röhl, I. Toudjarska, G. Wang, S. Wuschko, D. Bumcrot, V. Koteliansky, S. Limmer, M. Manoharan, H.-P. Vornlocher, *Nature* **2004**, *432*, 173–178.
[14] a) J. M. Layzer, A. P. Mccaffrey, A. K. Tanner, Z. Huang, M. A. Kay, B. A. Sullenger, *RNA* **2004**, *10*, 766–771; b) P. Dande, T. P. Prakash, N. Sioufi, H. Gaus, R. Jarres, A. Berdeja, E. E. Swayze, R. H. Griffey, B. Bhat, *J. Med. Chem.* **2006**, *49*, 1624–1634.
[15] O. Snøve, Jr., J. J. Rossi, *ACS Chem. Biol.* **2006**, *1*, 274–276.
[16] a) J. Martinez, A. Patkaniowska, H. Urlaub, R. Lurmann, T. Tuschl, *Cell* **2002**, *110*, 563–574; b) D. S. Schwarz, G. Hutvagner, B. Haley, P. D. Zamore, *Mol. Cell* **2002**, *10*, 537–548; c) Y.-L. Chiu, T. M. Rana, *Mol. Cell* **2002**, *10*, 549–561.
[17] A. Reynolds, D. Leake, Q. Boese, S. Scaringe, W. S. Marshall, A. Khvorova, *Nat. Biotechnol.* **2004**, *22*, 326–330.
[18] a) G. Hutvágner, M. J. Simard, C. C. Mello, P. D. Zamore, *Plos Biol.* **2004**, *2*, 465–475; b) S. L. Ameres, J. Martinez, R. Schroeder, *Cell* **2007**, *130*, 101–112.
[19] a) E. T. Kool, *Annu. Rev. Biophys. Biomol. Struct.* **2001**, *30*, 1–22; b) A. T. Krueger, E. T. Kool, *Curr. Opin. Chem. Biol.* **2007**, *11*, 588–594; c) A. P. Silverman, E. T. Kool, *J. Am. Chem. Soc.* **2007**, *129*, 10626–10627.
[20] A. Somoza, J. Chelliserrykattil, E. T. Kool, *Angew. Chem.* **2006**, *118*, 5116–5119; *Angew. Chem. Int. Ed.* **2006**, *45*, 4994–4997.
[21] J. Xia, A. Noronha, I. Toudjarska, F. Li, A. Akinc, R. Braich, M. Frank-Kamenetsky, K. G. Rajeev, M. Egli, M. Manoharan, *ACS Chem. Biol.* **2006**, *1*, 176–183.
[22] S. Pitsch, P. A. Weiss, L. Jenny, A. Stutz, X. Wu, *Helv. Chim. Acta* **2001**, *84*, 3773–3795.
[23] Q. Ji, J. Li, F. Huang, J. Han, J. Meng, *Synlett* **2005**, *8*, 1301–1305.
[24] Y. Xu, H-Y. Zhang, D. Thormeyer, O. Larsson, Q. Du, J. Elmén, C. Wahlestedt, Z. Liang, *Biochem. Biophys. Res. Commun.* **2003**, *306*, 712–717.
[25] G. Varani, W. H. McClain, *EMBO Rep.* **2000**, *1*, 18–23.
[26] S. Bommarito, N. Peyret, J. SantaLucia, *Nucleic Acids Res.* **2000**, *28*, 1929–1934.
[27] T. W. Kim, J. C. Delaney, J. M. Essigmann, E. T. Kool, *Proc. Natl. Acad. Sci. USA* **2005**, *102*, 15803–15808.
[28] F. Li, P. S. Pallan, M. A. Maier, K. G. Rajeev, S. L. Mathieu, C. Kreutz, Y. Fan, J. Sanghvi, R. Micura, E. Rozners, M. Manoharan, M. Egli, *Nucleic Acids Res.* **2007**, *35*, 6424–6438.
[29] Q. Du, H. Thonberg, J. Wang, C. Wahlestedt, Z. Liang, *Nucleic Acids Res.* **2005**, *33*, 1671–1677.
[30] H. O. Sintim, E. T. Kool, *Angew. Chem.* **2006**, *118*, 2008–2013; *Angew. Chem. Int. Ed.* **2006**, *45*, 1974–1979.
[31] J. Parsch, J. W. Engels, *Helv. Chim. Acta* **2000**, *83*, 1791–1808.

Received: May 2, 2008
Published online: July 15, 2008

